Full-wave three-dimensional microwave imaging with a regularized Gauss-Newton method

J. De Zaeytijd [1] **and A. Franchois** [2]

[1] INTEC, Ghent University
Sint-Pietersnieuwstraat 41, 9000 Ghent, Belgium
jurgen.dezaeytijd@intec.UGent.be
[2] INTEC - IMEC, Ghent University
Sint-Pietersnieuwstraat 41, 9000 Ghent, Belgium
ann.franchois@intec.UGent.be

Abstract: This paper treats the three dimensional full-wave inverse scattering problem. The goal is to reconstruct the complex permittivity within an investigation domain that is embedded in a homogeneous background medium. This reconstruction is treated as an optimization problem for the discretized permittivity profile only and no other unknowns are introduced. Therefore the fields in the investigation domain are eliminated from the problem by solving a multiview forward scattering problem in every step of the optimization whereby efficient algorithms such as the FFT-method and the marching-on-in-angle method are used. A Gauss-Newton optimization algorithm is applied to a new type of regularized cost function and yields rapid convergence. Several inversions from simulated data are presented.

Keywords: Microwave Imaging, , Inverse Scattering, Three Dimensional, Gauss-Newton Optimization, Regularization, Multiview Forward Problem, Complex Permittivity

1. Introduction

During the last two decades quantitative imaging techniques in the microwave region - providing reconstructions of electromagnetic parameters, such as permittivity and conductivity - were mainly developed for 2D configurations [1–6], mostly TM-polarized. The development of efficient forward and inverse scattering algorithms in the 2D framework, together with the advent of more powerfull PC's is now facilitating the transition to full-wave 3D quantitative imaging [2, 7–11].

Due to the non-linearity of the inverse scattering problem, an iterative reconstruction algorithm, in which a cost function is minimized, is mandatory. The scattered field depends on two types of unknowns, the complex permittivity and the total field inside the object, which are related by a domain integral equation constraint. With respect to these unkowns, most reconstruction methods can be divided in two categories. In the first, "conventional" approach, the total field unknown is eliminated from the problem, by means of solving a full forward problem in each iteration of the optimization algorithm, such that the cost function only depends on the complex permittivity [1–3, 5]. In the second "modified gradient" approach the domain integral equation constraint is added as a second term to the cost function, which is then minimized for both types of unknowns using a conjugate-gradient optimization scheme [4, 6, 8, 9]. In this contribution we have chosen to work with the conventional approach, which is implemented with an efficient forward solver and an efficient Gauss-Newton optimization procedure that converges very rapidly.

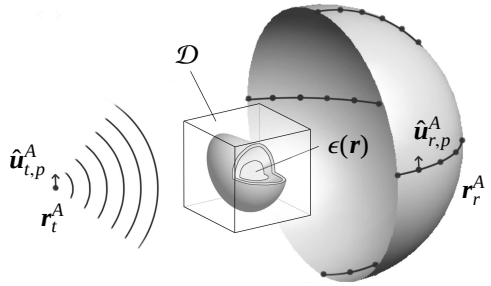

Figure 1: The 3D geometry for the inverse problem.

To handle the ill-posedness of the inverse scattering problem, a multiplicative-additive type of regularization is employed. This suppresses the effect of noise on the reconstructions and is believed to have its benefits in dealing with the non-linearity of the problem [16, 17].

Reconstructions from simulated data will be used to show the effectiveness of the proposed method.

2. Formulation of the Inverse Problem

Consider a 3D inhomogeneous lossy dielectric object situated in an infinite homogeneous and isotropic background (Fig. 1). For a fixed frequency $f = \omega/2\pi$ and from a number of transmitter points $\boldsymbol{r}^A_t$, $t = 1 \dots N^T$, the object is illuminated by electric dipoles oriented along the directions $\hat{\boldsymbol{u}}^A_{t,p}$, $p = 1 \dots N^P \leq 3$. For every such excitation, the scattered field is measured in the set of N^R_t receiver points $\boldsymbol{r}^A_r$, along the directions $\hat{\boldsymbol{u}}^A_{r,p}$, $p = 1 \dots N^P_t \leq 3$, where the set $\{r\}$ and possibly N^R_t can be different for each illumination t. The objective is to reconstruct the complex permittivity distribution $\epsilon(\boldsymbol{r}) = \epsilon'(\boldsymbol{r}) - j\epsilon''(\boldsymbol{r})$ within the volume $\mathcal{D}$ that encloses the object and that is sitting in a homogeneous background with permittivity ϵ_b.

It is well known that this inverse scattering problem is ill-posed, i.e. the existence, uniqueness and stability of the solution are not simultaneously guaranteed. Nonexistence is coped with by redefining the solution as the minimizer of a cost functional. Usually a least squares cost functional is applied:

$$F(\epsilon) = \frac{1}{F_0} \|\boldsymbol{e}^s(\epsilon) - \boldsymbol{e}^m\|^2, \tag{1}$$

where $\boldsymbol{e}^m$ is a vector that contains the data and $\boldsymbol{e}^s(\epsilon)$ contains the calculated values of the field, scattered by a permittivity distribution $\epsilon(\boldsymbol{r})$. The normalization factor F_0 is the squared norm of the data: $F_0 = \|\boldsymbol{e}^m\|^2$. Nonuniqueness is remedied by using "complete data", i.e. fields measured in points that form a good sampling of the sphere around $\mathcal{D}$ for a sufficient number of different illuminations. Finally the solution of the inverse scattering problem as the minimizer of (1) is known to be very sensitive to noise on the data. Because of this, a regularization of the problem is necessary and this will be discussed in more detail in section 5..

3. Contrast Source Integral Equation

A contrast source integral equation is used to describe the scattering from the inhomogeneous object when it is illuminated by an incident field $\boldsymbol{E}^{inc}(\boldsymbol{r})$ (the time dependency $e^{j\omega t}$ is omitted). Once the electric

field $\boldsymbol{E}(\boldsymbol{r})$ in the object is known, the scattered field $\boldsymbol{E}^{scat}(\boldsymbol{r})$ is calculated as the field, generated by the so-called contrast current, sitting in free space:

$$\boldsymbol{J}^{scat}(\boldsymbol{r}) = j\omega\left[\epsilon(\boldsymbol{r}) - \epsilon_b\right]\boldsymbol{E}(\boldsymbol{r}) = j\omega\chi(\boldsymbol{r})\boldsymbol{E}(\boldsymbol{r}), \tag{2}$$

$$\boldsymbol{E}^{scat}(\boldsymbol{r}) = -j\omega\mu_b\left[\mathbf{I} + \frac{1}{k_b}\nabla\nabla\right]\cdot\int_{\mathcal{D}} G_b(\boldsymbol{r}-\boldsymbol{r}')\boldsymbol{J}^{scat}(\boldsymbol{r}')\mathrm{d}\boldsymbol{r}', \tag{3}$$

where k_b is the background wavenumber and μ_b the background permeability. $G_b(\boldsymbol{r}-\boldsymbol{r}')$ is the Green function of the infinite background medium:

$$G_b(\boldsymbol{r}-\boldsymbol{r}') = \frac{e^{-jk_b\|\boldsymbol{r}-\boldsymbol{r}'\|}}{4\pi\|\boldsymbol{r}-\boldsymbol{r}'\|}. \tag{4}$$

To know the total field $\boldsymbol{E}(\boldsymbol{r})$ in $\mathcal{D}$ and thus the contrast currents, the following integral equation is solved

$$\boldsymbol{E}(\boldsymbol{r}) = \boldsymbol{E}^{inc}(\boldsymbol{r}) + \boldsymbol{E}^{scat}(\boldsymbol{r}),\ \forall\boldsymbol{r}\in\mathcal{D}, \tag{5}$$

which is referred to as the *domain equation*. Equation (3) is used to calculate the scattered field in the receiver points and is called the *observation equation*.

The inversion domain $\mathcal{D}$ is discretized using a uniform cuboidal grid of $F\times G\times H$ cells. On this grid, $\epsilon(\boldsymbol{r})$ is approximated by a piecewise constant function that has one value in each cuboidal cell:

$$\epsilon(\boldsymbol{r}) = \sum_{f=0}^{F-1}\sum_{g=0}^{G-1}\sum_{h=0}^{H-1}\epsilon_{f,g,h}\epsilon_b\Phi_{f,g,h}(\boldsymbol{r}), \tag{6}$$

where $\Phi_{f,g,h}(\boldsymbol{r}) = 1$ in cell (f,g,h) and zero elsewhere. As for the fields in the domain $\mathcal{D}$ that are needed in the forward problem, the electric flux density $\boldsymbol{D}(\boldsymbol{r}) = \epsilon(\boldsymbol{r})\boldsymbol{E}(\boldsymbol{r})$ rather than $\boldsymbol{E}(\boldsymbol{r})$ is expanded in 3D rooftop functions on the same grid or on a finer grid.

4. Multiview Forward Problem

To calculate the value of the cost function and its derivatives with respect to the permitivity unknowns, a multiview forward scattering problem has to be solved in every iteration of the optimization process: for every excitation along $\hat{\boldsymbol{u}}^A_{t,p}$ in $\boldsymbol{r}^A_t$ the field $\boldsymbol{E}_{t,p}(\boldsymbol{r})$ in $\mathcal{D}$ has to be known to calculate $\boldsymbol{E}^{scat}_{t,p}(\boldsymbol{r}^A_r)\cdot\hat{\boldsymbol{u}}^A_{r,p'}$. Also the derivatives of these fields with respect to the optimization parameters $\epsilon_{f,g,h}$ are needed for the optimization. Analytical expressions for the derivatives can be obtained

$$\frac{\partial\boldsymbol{E}^{scat}_{t,p}}{\partial\epsilon_{f,g,h}}(\boldsymbol{r}^A_r)\cdot\hat{\boldsymbol{u}}^A_{r,p'} = j\omega\epsilon_b\int_{\mathcal{D}}\Phi_{f,g,h}(\boldsymbol{r}')\boldsymbol{E}_{t,p}(\boldsymbol{r}')\cdot\boldsymbol{E}_{r,p'}(\boldsymbol{r}')\mathrm{d}\boldsymbol{r}', \tag{7}$$

where $\boldsymbol{E}_{r,p'}(\boldsymbol{r})$ is the field in $\mathcal{D}$ due to a dipole excitation along $\hat{\boldsymbol{u}}^A_{r,p'}$ in $\boldsymbol{r}^A_r$. This means that for every antenna, wether source or receiver, a forward problem must be solved. Since the solution of a full-vectorial 3D scattering problem is a computationally demanding task, two accelerating techniques are used. The *FFT method* [12–14] uses the convolution structure of (3) to accelarate the calculation of the scattered electric field in $\mathcal{D}$. In conjunction with an iterative solver this allows for rapid solution of (5). The *Marching on in Angle* method is an application of an extrapolation procedure described in [15]. The idea is to find a better initial estimate for the iterative solution of a linear system based on a number of previous solutions.

5. Regularization

To reduce the effect of noise on the reconstruction, we propose to minimize an alternative cost functional $F_R(\epsilon) = F(\epsilon)(1 + \alpha\sigma(\epsilon))$. The functional $\sigma(\epsilon)$ is always positive and penalizes strong local variations in the permittivity distribution. In discretized form it is given by

$$\sigma(\epsilon) = \sum_f \sum_g \sum_h \left(\left|\epsilon_{f,g,h} - \epsilon_{f-1,g,h}\right|^2 + \left|\epsilon_{f,g,h} - \epsilon_{f,g-1,h}\right|^2 + \left|\epsilon_{f,g,h} - \epsilon_{f,g,h-1}\right|^2 \right). \tag{8}$$

α is a positive real parameter that is chosen based on very general a priori knowledge, such as the maximal size of the object (already used to choose a domain $\mathcal{D}$) and an upper limit for the permittivity (already used to choose a mesh size for the forward problem). The fact that the regularization term is not only added to the least squares cost function, but also multiplied by it has a positive influence on the convergence and makes the choice of α less critical.

6. The Gauss-Newton Method

Let $\boldsymbol{\varepsilon}$ be the vector containing the coefficients $\epsilon_{f,g,h}$ from (6). Expressions for the gradient vector and the hessian matrix of the regularized cost function $F_R(\boldsymbol{\varepsilon}, \boldsymbol{\varepsilon}^*)$ as a function of $\boldsymbol{\varepsilon}$ and its complex conjugate $\boldsymbol{\varepsilon}^*$ are:

$$\boldsymbol{g}(\boldsymbol{\varepsilon}, \boldsymbol{\varepsilon}^*) = \begin{bmatrix} \frac{\partial F}{\partial \boldsymbol{\epsilon}} \\ \frac{\partial F}{\partial \boldsymbol{\epsilon}^*} \end{bmatrix} = \frac{1}{F_0} \begin{bmatrix} \boldsymbol{J}^T \left[\boldsymbol{e}^s - \boldsymbol{e}^m\right]^* (1 + \alpha\sigma) + \alpha F_0 F \boldsymbol{\Omega} \\ \boldsymbol{J}^H \left[\boldsymbol{e}^s - \boldsymbol{e}^m\right] (1 + \alpha\sigma) + \alpha F_0 F \boldsymbol{\Omega}^* \end{bmatrix} \tag{9}$$

$$\boldsymbol{H}(\boldsymbol{\varepsilon}, \boldsymbol{\varepsilon}^*) = \begin{bmatrix} \frac{\partial^2 F}{\partial \boldsymbol{\epsilon} \partial \boldsymbol{\epsilon}} & \frac{\partial^2 F}{\partial \boldsymbol{\epsilon} \partial \boldsymbol{\epsilon}^*} \\ \frac{\partial^2 F}{\partial \boldsymbol{\epsilon}^* \partial \boldsymbol{\epsilon}} & \frac{\partial^2 F}{\partial \boldsymbol{\epsilon}^* \partial \boldsymbol{\epsilon}^*} \end{bmatrix} = \frac{1}{F_0} \begin{bmatrix} \boldsymbol{B}' & \boldsymbol{A}^* \\ \boldsymbol{A} & \boldsymbol{B}'^* \end{bmatrix}, \tag{10}$$

with

$$\boldsymbol{B}' = B(1 + \alpha\sigma) + \alpha \boldsymbol{J}^T \left[\boldsymbol{e}^s - \boldsymbol{e}^m\right]^* \boldsymbol{\Omega}^T + \alpha \boldsymbol{\Omega} \left[\boldsymbol{e}^s - \boldsymbol{e}^m\right]^T \boldsymbol{J} \tag{11}$$

$$\boldsymbol{A} = \boldsymbol{J}^H \boldsymbol{J}(1 + \alpha\sigma) + \alpha \boldsymbol{J}^H \left[\boldsymbol{e}^s - \boldsymbol{e}^m\right] \boldsymbol{\Omega}^T + \alpha \boldsymbol{\Omega}^* \left[\boldsymbol{e}^s - \boldsymbol{e}^m\right]^H \boldsymbol{J} + \alpha F_0 F \boldsymbol{\Sigma} \tag{12}$$

and where

$$J_{ij} = \frac{\partial e_i^s}{\partial \epsilon_j}, \quad B_{ij} = \left(\frac{\partial^2 \boldsymbol{e}^s}{\partial \epsilon_i \partial \epsilon_j} \right)^T \left[\boldsymbol{e}^s - \boldsymbol{e}^m\right]^*, \quad \Sigma_{ij} = \frac{\partial^2 \sigma}{\partial \epsilon_i \partial \epsilon_j^*} \quad \text{and} \quad \Omega_i = \frac{\partial \sigma}{\partial \epsilon_i}. \tag{13}$$

Linearizing the scattered field $\boldsymbol{E}^{scat}$, as a function of the permittivity-vector $\boldsymbol{\varepsilon}$, around the current iterate $\boldsymbol{\varepsilon}_k$ and applying Newton's method with some additional simplifications, one gets following update formula:

$$\boldsymbol{\varepsilon}_{k+1} - \boldsymbol{\varepsilon}_k = \Delta\boldsymbol{\varepsilon} = -\left(\boldsymbol{J}^H \boldsymbol{J}(1 + \alpha\sigma) + \alpha F_0 F \boldsymbol{\Sigma} \right)^{-1} \left(\boldsymbol{J}^H \left[\boldsymbol{e}^s - \boldsymbol{e}^m\right] (1 + \alpha\sigma) + \alpha F_0 F \boldsymbol{\Omega}^* \right), \tag{14}$$

where all the quantaties in the right hand side are calculated for $\boldsymbol{\varepsilon}_k$. In practice, this update vector is used as a search direction along which a line search is performed to find the next iterate. Together with the fact that (14) always produces descent directions, this ensures decreasing values of the cost function.

It can be argued that the effect of the regularization term $\alpha F \sigma$ on the optimization process is the following: it improves the conditioning of the linear system (14), it bounds the update directions away from orthogonality to the steepest descent direction, it controls the smoothness of the permittivity profile in every iteration and it controls the steplength. The latter effect improves the validity of the linearization of the scattered field.

7. Numerical Examples

Figure 2 shows the reconstruction of a homogeneous dielectric sphere with radius $0.25\lambda_b$ an with $\epsilon = 2\epsilon_b$. The antenna configuration for this example consists of 6 meridional circular arrays, centered on the center of the sphere, with a radius $R = \lambda_b$ and each containing 12 antennas in azimuthal directions and 12 antennas along the meridional circle. All antennas act as both transmitter and receiver, so a total number of 20736 datapoints is obtained. The data are generated by analytical solution of the forward scattering problem. For the inversion domain a cube with side λ_b is chosen, which is discretized using $20 \times 20 \times 20 = 8000$ permittivity cells. The discretization noise results in an SNR of 27 dB. When the squared data error or the least squares cost function F (see (1)) reaches $F \leq 2 \cdot 10^{-3}$, which corresponds to the noise level, the optimization is stopped. With a regularization parameter $\alpha = 10^{-4}$ the result is obtained in only three iterations and within 73 minutes on a computer with 2 GHz Dual Core AMD Opteron processor and 8 Gbytes of RAM.

A second example is the reconstruction of the permittivity profile, shown in Figure 3. The background medium is water with a permittivity of $\epsilon_w = (77.3 - j21.2)\epsilon_0$ at 1 GHz. A cube with side $0.6\lambda_b$ and permittivity $\epsilon_f = (9.5 - j7.19)\epsilon_0$ (fatty tissue) is submersed in this medium. Inside this cube is a smaller one with tumor-like properties $\epsilon_t = (50 - j71.9)\epsilon_0$. The result is a highly contrasted permittivity profile which is not easy to reconstruct. The antenna configuration now consists of 6 meridional circular arrays, centered on the center of the sphere, with a radius $R = 2\lambda_b$ and each containing 12 antennas along the meridional circle, which results in 5184 datapoints. Figure 4 shows the reconstruction for an SNR of 50 dB and Figure 5 corresponds to an SNR of 30 dB. Both reconstructions were obtained with $\alpha = 5 \cdot 10^{-4}$.

8. Conclusions

A modified Gauss-Newton method has been proposed to solve the three dimensional inverse scattering problem. It minimizes a regularized cost function and provides good reconstructions after only a small number of iterations. As a consequence, the total execution time of the algorithm remains reasonable, even though in every step of the optimization a full multiview forward problem is solved. Numerical examples were shown to prove the validity of the method and to illustrate its performance.

References

[1] W.C. Chew, Y.M. Wang, "Reconstruction of Two-Dimensional Permittivity Distribution Using the Distorted Born Iterative Method", *IEEE Trans. Medical Imaging*, Vol. 9, No. 2, pp. 218 - 225, 1990.

[2] N. Joachimowicz, C. Pichot, J. Hugonin, "Inverse Scattering: An Iterative Numerical Method for Electromagnetic Imaging", *IEEE Trans. Antennas Propagat.*, Vol. 39, No. 12, pp. 1742-1752, 1991.

[3] A. Franchois, C. Pichot, "Microwave Imaging - Complex Permittivity Reconstruction with a Levenberg-Marquardt Method", *IEEE Trans. Antennas Propagat.*, Vol. 45, No. 2, pp. 203-215, 1997.

[4] P.M. van den Berg, R.E. Kleinman, "A Contrast Source Inversion Method", *Inverse Problems*, Vol. 13, No. 6, pp. 1607-1620, 1997.

[5] A. Franchois, A.G. Tijhuis, "A Quasi-Newton Reconstruction Algorithm for a Complex Microwave Imaging Scanner Environment", *Radio Science*, Vol. 38, No. 2, 2003.

[6] A. Abubakar, T.M. Habashy, P.M. van den Berg, D. Gisolf, "The Diagonalized Contrast Source Approach: an inversion method beyond the Born approximation", *Inverse Problems*, Vol. 21, No. 2, pp. 685-702, 2005.

[7] A.E. Bulyshev, A.E. Souvorov, S.Y. Semenov, R.H. Svenson, A.G. Nazarov, Y.E. Sizov, G.P. Tatsis, "Three-Dimensional Microwave Tomography. Theory and Computer Experiments in Scalar Approximation", *Inverse Problems*, Vol. 16, No. 3, pp. 863-875,2000.

[8] A. Abubakar, P.M. van den Berg, J.J. Mallorqui, "Imaging of Biomedical Data Using a Multiplicative Regularized Contrast Source Inversion Method", *IEEE Trans. Microwave Theory and Techniques*, Vol. 50, No. 7, pp. 1761-1770, 2002.

[9] Z.Q. Zhang, Q.H. Liu, "Three-Dimensional Nonlinear Image Reconstruction for Microwave Biomedical Imaging", *IEEE Trans. Biomedical Engineering*, Vol. 51, No. 3, pp. 544-548, 2004.

[10] G. Franceschini, D. Franceschini, A. Massa, "Full-Vectorial Three-Dimensional Microwave Imaging through the Iterative Multiscaling Strategy - A Preliminary Assessment" ,*IEEE Geoscience and Remote Sensing Letters*, Vol. 2, No. 4, pp. 428-432, 2005.

[11] K. Belkebir, P.C. Chaumet, A. Sentenac, "Influence of Multiple Scattering on Three-Dimensional Imagig with Optical Diffraction Tomography", *J. Opt. Soc. Am. A.*, Vol. 23, No. 3, pp. 586-595,2006.

[12] T.K. Sarkar, E. Sarvas, S.M. Rao, "Application of FFT and the Conjugate Gradient Method for the Solution of Electromagnetic Radiation from Electrically Large and Small Conductinb Bodies", *IEEE Trans. Antennas Propagat.*, Vol. 34, No. 5, pp. 635-640, 1986 .

[13] P. Zwamborn, P.M. van den Berg, "The Three-Dimensional Weak Form of the Conjugate Gradient FFT Method for Solving Scattering Problems", *IEEE Trans. Microwave Theory and Techniques*, Vol. 40, No. 9, pp. 1757-1766, 1992.

[14] H. Gan, W.C. Chew, "A Discrete BCG-FFT Algorithm for Solving 3D Inhomogeneous Scatterer Problems", *IEEE Trans. Antennas Propagat.*, Vol. 9, No. 10, pp. 1339-1357, 1995.

[15] A.G. Tijhuis, M.C. van Beurden, A.P.M. Zwamborn, "Iterative Solution of Field Problems with a Varying Physical Parameter", *Turk. J. Elec. Engin.*, Vol. 10, No. 2, pp. 163-183, 2002.

[16] J. De Zaeytijd, A. Franchois, C. Eyraud, J.M. Geffrin, "Three Dimensional Complex Permittivity Reconstruction by Means of Newton-Type Microwave Imaging", *Proceedings of EUCAP 2006*, 6-10 November 2006, Nice, France, CD-ROM, session OA13, 6 p.

[17] P. Lewyllie, J. De Zaeytijd and A. Franchois, "Quantitative microwave imaging of 3D inhomogeneous objects," *2006 USNC/URSI National Radio Science Meeting, held in conjunction with the IEEE Antennas and Propagation Society International Symposium*, 9-14 July 2006, Albuquerque, USA, p. 177.

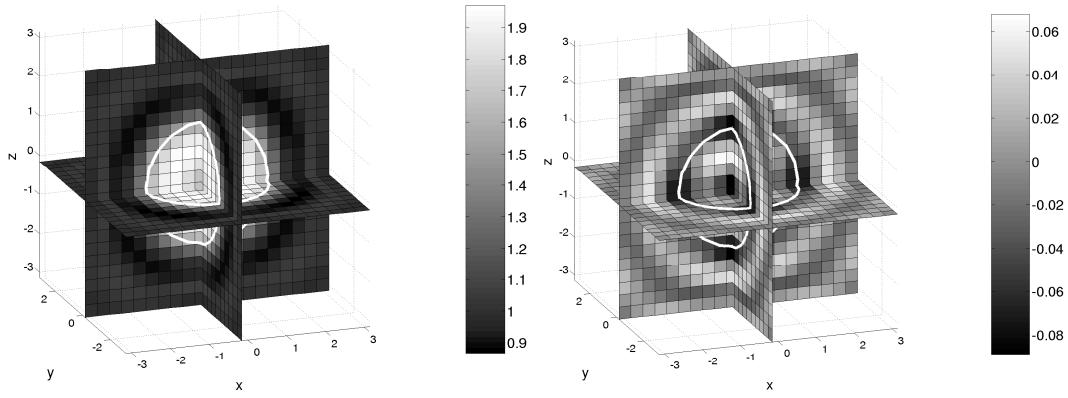

(a) Real part of ϵ-profile. (b) Imaginary part of ϵ-profile.

Figure 2: Reconstruction of a sphere with radius $0.25\lambda_b$ from analytic data. The white contour shows the boundaries of the actual sphere.

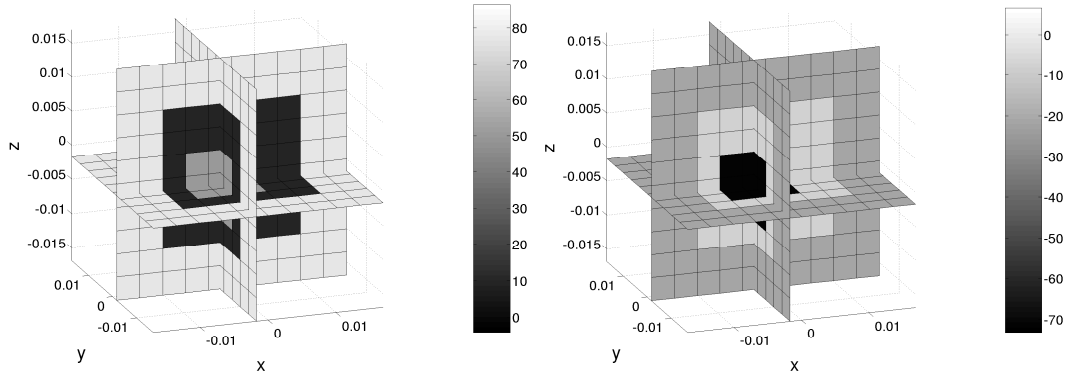

(a) Real part (b) Imaginary part

Figure 3: The exact permittivity profile. The plotted values are $\epsilon(\boldsymbol{r})/\epsilon_0$.

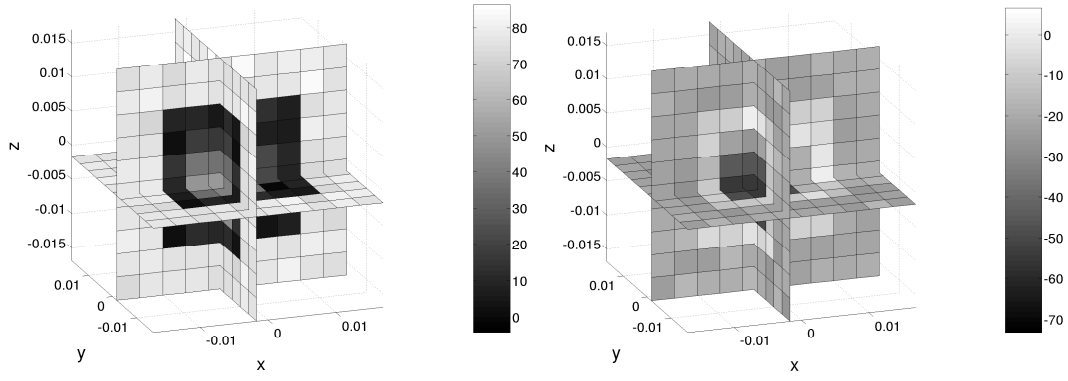

(a) Real part (b) Imaginary part

Figure 4: The reconstructed permittivity profile for an SNR of 50 dB.

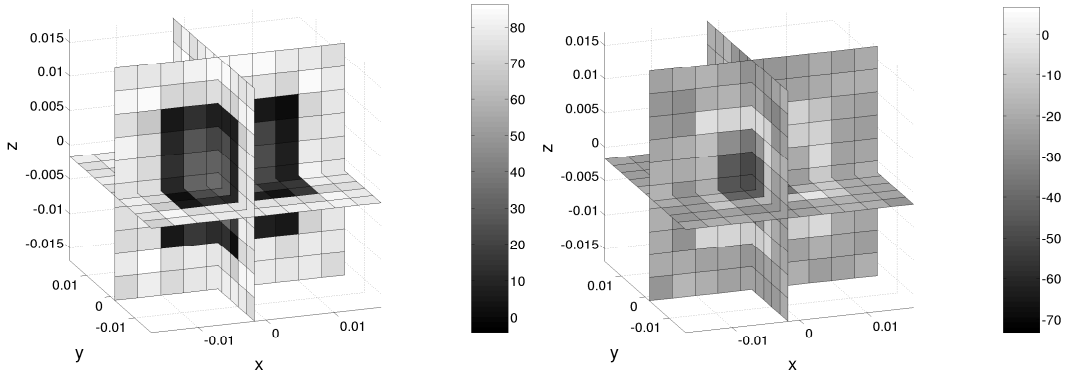

(a) Real part (b) Imaginary part

Figure 5: The reconstructed permittivity profile for an SNR of 30 dB.